

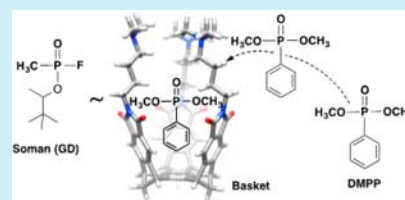
## Ubiquitous Assembly of Amphiphilic Baskets into Unilamellar Vesicles and Their Recognition Characteristics

Yian Ruan, Shigui Chen, Jason D. Brown, Christopher M. Hadad, and Jovica D. Badjić\*

Department of Chemistry and Biochemistry, The Ohio State University, 100 West 18th Avenue, Columbus, Ohio 43210, United States

## Supporting Information

**ABSTRACT:** An amphiphilic basket of type 1 (339 Å<sup>3</sup>) has been found to assemble into unilamellar vesicles in water. The assembled host encapsulates organophosphonates (OPs) (119–185 Å<sup>3</sup>) with a particularly high affinity ( $K_a \sim 10^5 \text{ M}^{-1}$ ) toward dimethyl phenylphosphonate (185 Å<sup>3</sup>) whose size and shape resemble that of soman (186 Å<sup>3</sup>). Importantly, the entrapment of OPs prompts a phase transformation of vesicular 1 into nanoparticles or larger vesicles as a function of the shape of the host–guest complex.



Chemical warfare agents of the *G* and *V* types are organophosphorus (OP) compounds containing an electrophilic phosphorus atom surrounded by four substituents of which one is a good leaving group.<sup>1</sup> These reactive molecules are tetrahedral in shape and relatively small (132–289 Å<sup>3</sup>) and can fit in the active site of acetylcholinesterase (AChE), where they react with a nucleophilic serine residue to covalently inhibit the enzyme.<sup>2</sup> Consequently, the hydrolysis of neurotransmitter acetylcholine is suppressed to prompt the hyperactivity of cholinergic nerves, muscles, and glands.<sup>3</sup> In the case of overdose, however, the poisoning leads to respiratory failure and death.<sup>4</sup> To date, the unambiguous detection of nerve agents remains a challenging task and requires the use of nonportable analytical equipment.<sup>1</sup> A potential solution may involve the development of inexpensive, yet efficient/selective, chemosensors.<sup>5</sup> For the removal of OP compounds from exposed areas and humans, however, one could employ biological or supramolecular catalysts (or scavengers)<sup>6</sup> capable of promoting the rapid hydrolysis (or isolation) of these toxic substances.<sup>1,7</sup> Despite steady progress in the development of such compounds,<sup>8</sup> many issues remain to be addressed, including control of substrate selectivity and reaction rates as well as the persistence and stability of catalysts/scavengers. Accordingly, we recently started a research program with an aim of developing a series of basket-like compounds<sup>9</sup> capable of selectively complexing small organophosphonates that are similar in size and shape to authentic chemical nerve agents.<sup>10</sup> Thus far, novel molecular baskets have been designed to comprise a concave cup to which amino acids<sup>11</sup> or amphiphilic chains<sup>12</sup> are conjugated. These artificial hosts possess a millimolar or higher affinity for encapsulating various organophosphonates (132–289 Å<sup>3</sup>) in water, with the “classical” hydrophobic effect<sup>13</sup> playing an important role in the OP recognition. In particular, amphiphilic baskets with a large cavity ( $V = 477 \text{ Å}^3$ ) were found<sup>12</sup> to assemble into unilamellar vesicles, which upon trapping a particular OP compound, morphed into nanoparticles or larger vesicles:<sup>14</sup> the phase transformation is a function of the structure of the host–guest complex (i.e., its shape) undergoing the aggregation. These earlier findings begged a question: will

amphiphilic baskets of type 1, containing a shallow cup-shaped cavity (Figure 1,  $V = 339 \text{ Å}^3$ ), also assemble in water to give

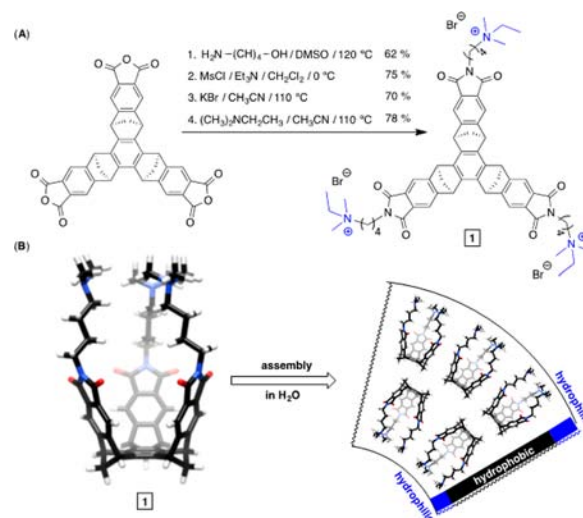


**Figure 1.** (A) Synthesis of basket 1. (B) Energy-minimized (MMFFs) conformer of amphiphilic 1 (left) and schematic representation of its packing into a vesicular bilayer (right).

vesicles capable of complexing OPs (Figure 1B)? What characteristics will best describe the encapsulation and assembly of such [1Cguest] complexes? To address these questions, we prepared basket 1 and then studied its aggregation characteristics and the complexation of several OPs in water.

To prepare amphiphilic 1 (Scheme S1, Supporting Information), we followed a strategy described in Figure 1A.<sup>12</sup> Thus, the condensation of 4-amino-1-butanol with tris-anhydride yielded tris-alcohol, which was subjected to mesylation for introducing

Received: December 20, 2014

Published: February 5, 2015

good leaving groups into the substrate. Nucleophilic substitution with bromide in acetonitrile followed by the addition of *N*-ethyl-*N,N*-dimethylamine provided basket **1** in overall 25% yield (Figure 1A). Importantly,  $C_{3v}$ -symmetric **1** is amphiphilic with a hydrophobic cup at its southern terminus and three hydrophilic ammonium cations at the northern side (Figure 1B). The conformational characteristics of this cavitant were elucidated with a Monte Carlo computational search, followed by a series of molecular dynamics (MD, AMBER) simulations in explicit water solvent.<sup>10</sup> On the basis of the clustering analysis (Figure 2A), the

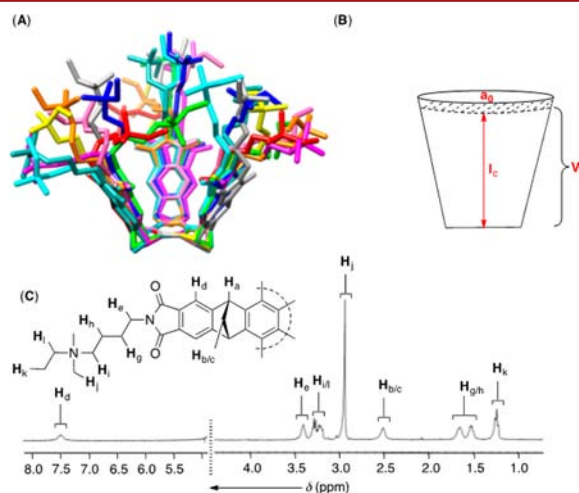


**Figure 2.** (A) Ten representative conformers of basket **1** were obtained from an MD (AMBER) study in  $H_2O$ , followed by clustering analysis of the computed MD trajectories. (B) The geometric characteristics of the 10 conformers of **1** (resembling a truncated cone) were estimated to give  $V = 814 \text{ \AA}^3$ ,  $l_c = 9.1 \text{ \AA}$ , and  $a_0 = 193 \text{ \AA}^2$  so that  $P = V/(a_0 l_c) \sim 0.5$ . (C)  $^1H$  NMR spectrum (400 MHz) of amphiphilic **1** (1.0 mM) in  $D_2O$  at 300.0 K.

basket is predicted to adopt the shape of a truncated cone (Figure 2B). The three aliphatic chains at the rim extend into polar water solution to create a preorganized and “hydrophobic pocket” for accommodating a tetrahedral organophosphonate guest. The cavitant should, on the basis of the Israelachvili’s semiempirical rules,<sup>15</sup> pack into vesicular assemblies.<sup>16</sup> That is to say, we estimated the geometric characteristics of 10 preferred conformers of **1** and then computed the so-called packing factor  $P = v/(a_0 l_c)$  to be  $\sim 0.5$  (Figure 2B). This dimensionless number describes the aggregation mode of amphiphiles: when  $0.5 < P < 1$  and the concentration of the amphiphile is greater than the critical vesicle concentration (CVC, see below), the packing into vesicles ensues.<sup>15</sup> In line with the prediction, basket **1** was found to be soluble in  $D_2O$  (from 0.05 to 1.0 mM at 300.0 K; Figure S1, Supporting Information), although the basket showed a set of broad  $^1H$  NMR resonances corresponding to a  $C_3$ -symmetric compound (Figure 2C). In essence, the aggregation of **1** could lead to the broadening  $^1H$  NMR spectroscopic signals due to (a) shorter  $T_2$  relaxation times of its proton nuclei and/or (b) exchange processes occurring at intermediate rates.<sup>12</sup> To more closely inspect the noncovalent association of **1**, we completed a series of transmission electron microscopy (TEM, Figure 3) measurements of an aqueous solution of **1** (1.0 mM) deposited on copper grids. As originally anticipated, amphiphilic **1** formed vesicles with spherical morphology and an approximate diameter of 250 nm (Figure 3A). Given that TEM sample preparation could enable the aggregation of **1** (i.e., the evaporation of  $H_2O$

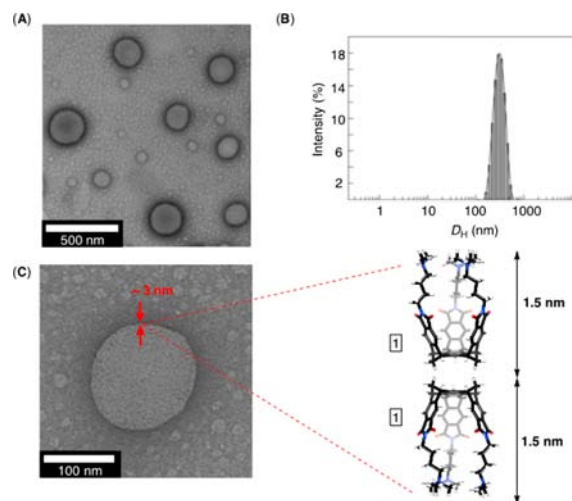


**Figure 3.** (A) TEM image of **1** (1.0 mM in  $H_2O$ ) deposited on a copper grid and stained with uranyl acetate. (B) Plot showing the size distribution of the assembled particles in a solution of **1** (1.0 mM in  $H_2O$ ) as examined with dynamic light scattering (DLS) at 298.0 K; the hydrodynamic diameter is centered at  $D_H \sim 295 \text{ nm}$  with polydispersity index of  $PDI = 0.40$ . (C) Enlarged TEM image of **1** (1.0 mM in  $H_2O$ ) deposited on a copper grid and stained with uranyl acetate. The thickness of the vesicular membrane is estimated to be 3 nm, corresponding to the length of two baskets (each 1.5 nm, MMFFs).

solvent on copper grids), we used dynamic light scattering (DLS) to additionally examine its 1.0 mM solution (Figure 3B). Evidently, basket **1** (1.0 mM) aggregates into nanosized particles with a distribution of hydrodynamic diameters centered at  $D_H = 295 \text{ nm}$ . The result is in agreement with our TEM measurements, thereby corroborating the formation of vesicular **1** in  $H_2O$ ! Next, we “zoomed” in on a single vesicle of **1** (TEM, Figure 3C) to estimate the thickness of its membrane to be  $\sim 3 \text{ nm}$ . The width corresponds to two amphiphilic baskets (each 1.5 nm) forming a bilayer boundary to separate the vesicle’s aqueous reservoir from the bulk solvent. Finally, we titrated amphiphilic **1** (5.0 mM) into neat  $H_2O$  and followed the change in heat accompanying the process using isothermal titration calorimetry (ITC, Figure S2, Supporting Information):<sup>17</sup> vesicular **1** could, upon dilution, (a) break down into solvated “free” molecules or (b) retain its original morphology. For the concentration range of  $33 \mu\text{M}$  to 1.4 mM, however, the experimental isotherm showed no abrupt transitions (Figure S2, Supporting Information), suggesting that the critical vesicle concentration (CVC) of amphiphilic **1** is lower than  $33 \mu\text{M}$ .<sup>18</sup>

We recently found that baskets with three amino acid groups at the rim, instead of aliphatic chains in **1** (Figure 1),<sup>10</sup> possess a greater affinity for encapsulating dimethyl methylphosphonate **2** (Figure 4) than larger OPs ( $>119 \text{ \AA}^3$ ). In particular, an OP guest was determined to place its  $P-CH_3$  group inside the aromatic cup of the host.<sup>19</sup> To test the encapsulation characteristics of vesicular **1** ( $339 \text{ \AA}^3$ ), we used  $^1H$  NMR spectroscopy as well as calorimetry to quantify the host’s affinity for trapping of **2–7** in water (Figure 4). These OP guests vary in size and charge, with **2–4** being smaller ( $72–119 \text{ \AA}^3$ ) and **5–7** being larger ( $138–185 \text{ \AA}^3$ ). Interestingly, we found that **2** and **5–7** would occupy the inner space of **1** ( $^1H$  NMR spectroscopy, Figures S3–S6, Supporting Information), while **3** and **4** have no measurable affinity toward the amphiphilic host. The binding stoichiometry was, for the formation of  $[1C5]$ , confirmed by a Job plot (Figure S10, Supporting Information), while in other cases, the nonlinear

	<b>2</b>	<b>3</b>	<b>4</b>	<b>5</b>	<b>6</b>	<b>7</b>
Size (Å <sup>3</sup> )	119	95	72	185	161	138
$K_a$ (M <sup>-1</sup> )	NMR 447 ± 8 ITC 457 ± 16	—	—	6742 ± 323 9017 ± 922	1259 ± 71 3259 ± 216	155 ± 4
$\Delta H^\circ$ (kcal/mol)	-3.48 ± 0.04	—	—	-4.09 ± 0.08	-1.03 ± 0.02	—
$-T\Delta S^\circ$ (kcal/mol)	-0.15 ± 0.06	—	—	-1.31 ± 0.15	-3.76 ± 0.06	—
$\Delta G^\circ$ (kcal/mol)	-3.63 ± 0.07	—	—	-5.4 ± 0.2	-4.79 ± 0.06	—

**Figure 4.** <sup>1</sup>H NMR spectroscopy (Figures S3–S6, Supporting Information) and isothermal titration calorimetry (ITC, Figures S7–S9, Supporting Information) were used to determine thermodynamic parameters characterizing the complexation of organophosphonates 2–7 (72–185 Å<sup>3</sup>) with amphiphilic basket **1** to give the corresponding [1Cguest] complex in water at 300.0 K (NMR) and 298.0 K (ITC).

least-squares analysis of NMR titration data would fit well to a model describing the formation of 1:1 host–guest complexes (Figures S3–S6, Supporting Information).<sup>20</sup> In the case of neutral guests **2** and **5**, the complexation is driven by favorable enthalpy ( $\Delta H^\circ < -3.5$  kcal/mol, Figure 4), while with anionic **6**, the entropy ( $-T\Delta S^\circ < -3.5$  kcal/mol, Figure 4) dominates the free energy of binding ( $\Delta G^\circ$ , 298.0 K).<sup>14</sup> Presumably, a hydrophobic effect is operating in all encapsulation events (via desolvation of hydrophobic surfaces),<sup>13</sup> although noncovalent host–guest interactions of van der Waals, C–H... $\pi$  and  $\pi$ ... $\pi$  type make a considerable contribution ( $\Delta H^\circ < -3.5$  kcal/mol, Figure 4) to the complexation thermodynamics of neutral OPs.<sup>14</sup> Lastly, the larger the guest the more favorable the complexation albeit anionic guests possess a lower propensity for populating the inner space of cationic **1** (Figure 4)! In retrospect, the shape and electronic complementarity<sup>21</sup> of the host–guest pair could be a critical factor in determining the thermodynamic stability of the observed complexes. Accordingly, why would neutral OPs constitute a better fit to amphiphilic **1** than the corresponding anionic ones? After all, previously studied amphiphilic baskets,<sup>14</sup> with a more sizable inner space, were found to have a greater affinity for anionic than neutral OPs.

To more closely inspect the structure of [1Cguest] complexes, we generated plots (Figure 5A/B) showing the normalized change in the chemical shifts of <sup>1</sup>H NMR signals of guests 2/5–7 ( $\Delta\delta^* = \delta_{\text{observed}} - \delta_{\text{bound}}^*$ ) as a function of their increased concentration in a standard D<sub>2</sub>O solution of basket **1** (1.0 mM); note that the apparent  $\delta_{\text{bound}}^*$  (Figure 5A/B) corresponds to the measured NMR chemical shift of the guest at the first titration point so that, in each case, the dependence would originate at  $\Delta\delta^* = 0$ . The signals corresponding to O–CH<sub>3</sub> and P–CH<sub>3</sub> protons, within neutral guests **2** and **5**, showed an upfield shift within [1C2]/[1C5] complexes (Figure 5A). Accordingly, these groups reside in the shielded region of the aromatic cup-shaped platform of **1**. A greater perturbation of the O–CH<sub>3</sub> resonances ( $\Delta\delta^* = 0.5$ –1 ppm, Figure 5A), however, suggests that the methoxy groups of neutral guests **2** and **5** are primarily occupying the host's aromatic cup. Compounds **2** and **5** are therefore complementary to the cone-shaped **1** when positioning one of their O–CH<sub>3</sub> groups in the host's cavity. It follows that removal of one or both of the methoxy groups should lower the thermodynamic stability of the corresponding complexes due to a reduced host–guest complementarity.<sup>22</sup> Indeed, anionic 3/4 and 6/7 were found to possess a lower affinity for complexing basket **1** than neutral **2** and **5**, respectively (Figure 4)! Along with this logic, anionic guests **6** and **7** position their P–C<sub>6</sub>H<sub>5</sub> moiety in the cavity of **1**, since the resonances corresponding to benzene H<sub>a/b/c</sub>

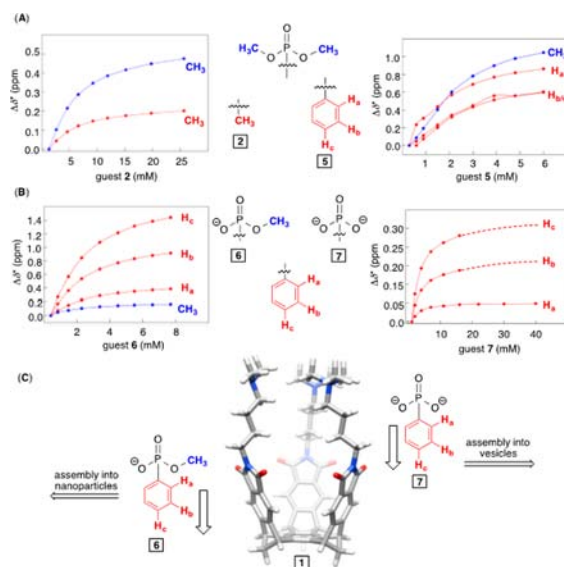


**Figure 5.** (A, B) Normalized <sup>1</sup>H NMR chemical shifts ( $\Delta\delta^* = \delta_{\text{observed}} - \delta_{\text{bound}}^*$ ) of proton resonances in **2**, **5**, **6**, and **7** as a function of their increasing concentration in 1.0 mM solution of **1** in D<sub>2</sub>O. (C) Organophosphonates **6** and **7**, containing Na<sup>+</sup> counterion(s), occupy the cavity of **1**, each with its H<sub>c</sub> proton pointing to the basket's aromatic "floor". Apparently, monoanionic **6** (left) inserts deeper in the cavity of **1** than dianionic **7** (right).

protons in **6** show a greater degree of magnetic perturbation ( $\Delta\delta^*$ , Figure 5B) than the OCH<sub>3</sub> signal. Furthermore, H<sub>c</sub> protons of both **6** and **7** ought to be situated deeper in the cavity of the host than H<sub>a</sub> protons as the degree of diamagnetic shielding is in order of H<sub>c</sub> > H<sub>b</sub> > H<sub>a</sub> (Figure 5B). While both anionic guests occupy basket **1** with their benzene moiety pointing to the host's aromatic "floor" (Figure 5C), there still remains a question about the degree of their inclusion. That is to say, which of two guests, **6** or **7**, is located deeper in the cavity of **1**, if any? To obtain  $\Delta\delta = \delta_{\text{free}} - \delta_{\text{bound}}$  for H<sub>c</sub> of **6** and **7**, and therefore evaluate the degree of inclusion of these two compounds, we decided to calculate the chemical shift of H<sub>c</sub> corresponding to fully complexed guests ( $\delta_{\text{bound}}^*$ ).<sup>23</sup> Thus, using the chemical shift of free guest ( $\delta_{\text{free}}(\mathbf{6}) = 7.52$  ppm,  $\delta_{\text{free}}(\mathbf{7}) = 7.32$  ppm), the association constant  $K_a$  for the formation of [1C6/7] complex ( $K_a(\mathbf{6}) = 1259$  M<sup>-1</sup> and  $K_a(\mathbf{7}) = 155$  M<sup>-1</sup>, Figure 4), the observed chemical shifts of the guest in solution ( $\delta_{\text{observed}}(\mathbf{6}) = 5.69$  ppm at  $[\mathbf{6}]_0 = 0.42$  mM,  $\delta_{\text{observed}}(\mathbf{7}) = 7.05$  ppm at  $[\mathbf{7}]_0 = 1.0$  mM with  $[\mathbf{1}]_0 = 1.0$  mM) and the relationship  $\delta_{\text{observed}} = \delta_{\text{free}}f_{\text{free}} + \delta_{\text{bound}}f_{\text{bound}}$  we calculated that  $\delta_{\text{bound}}$  for **6** is 3.87 ppm while for **7** is equal to 5.05 ppm; note that the fractions of bound guest ( $f_{\text{free}} + f_{\text{bound}} = 1$ ), calculated from the NMR binding constants, are  $f_{\text{bound}}(\mathbf{6}) = 0.50$  and  $f_{\text{bound}}(\mathbf{7}) = 0.12$ . It follows that  $\Delta\delta = \delta_{\text{free}} - \delta_{\text{bound}}$  for the H<sub>c</sub> proton is greater in **6** (3.6 ppm) than in **7** (2.3 ppm), indicating a more considerable magnetic perturbation of this nucleus in [1C6] than [1C7] complex. With monoanionic guest **6** penetrating the cavity of **1** to a greater extent, we reason that there should be a greater expansion of the host's cup-shaped platform.<sup>10</sup> On the contrary, dianionic guest **7** is occupying the cavity of **1** to a lesser degree with the shape of [1C7], we posit, similar to that of the free basket. Importantly, a change in the shape of host–guest complexes was previously shown<sup>12,14</sup> to affect their mode of aggregation. Accordingly, we deduced that [1C6] could assemble into nanoparticles while [1C7], resembling vesicular **1** in shape, should transform into vesicles. Indeed, the results of TEM and



DLS measurements (Figure 6) confirmed our prediction. Thus, vesicular **1** complexed guest **6** to change into nanoparticles with a

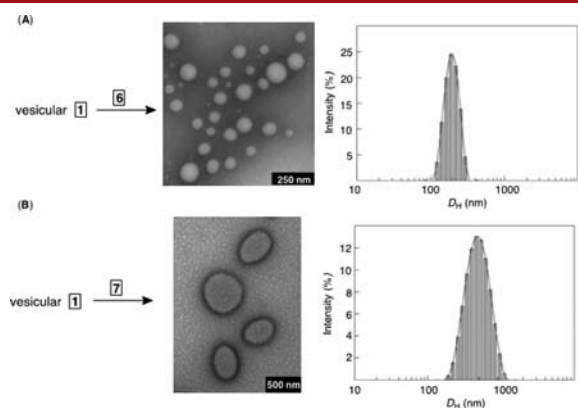


**Figure 6.** (A) TEM image of amphiphilic **1** (1.0 mM in H<sub>2</sub>O) containing **6** (7.7 mM) and a plot showing the size distribution of the assembled particles in a solution of **1** (1.0 mM in H<sub>2</sub>O) containing **6** (7.7 mM) as examined with DLS at 298.0 K. (B) TEM image of amphiphilic **1** (1.0 mM in H<sub>2</sub>O) containing **7** (40.0 mM) and a plot showing the size distribution of the assembled particles in a solution of **1** (1.0 mM in H<sub>2</sub>O) containing **7** (40.0 mM) as examined with DLS at 298.0 K.

diameter of 100–200 nm (Figure 6A). On the contrary, the encapsulation of dianionic organophosphonate **7** by **1** gave rise to complex [1C7], similar in shape to the basket itself, so that vesicles consisting of **1** ( $D_H \sim 250\text{--}300$  nm, Figure 3) merely packed into more sizable vesicles ( $D_H \sim 450$  nm, Figure 6B).

In conclusion, we have found that amphiphilic baskets of type **1** with a smaller inner space ( $339 \text{ \AA}^3$ ) assemble into unilamellar vesicles in water.<sup>24</sup> The vesicular host is complementary to dimethyl phenylphosphonate **5** ( $185 \text{ \AA}^3$ ) placing its O–CH<sub>3</sub> group in the cavity of the host. Markedly, amphiphilic basket **1** has a considerable affinity for trapping **5**, similar in size and shape to soman ( $186 \text{ \AA}^3$ ,  $K_a \sim 10^5 \text{ M}^{-1}$  at 298.0 K in H<sub>2</sub>O). Importantly, the complexation of OP guests is accompanied by a change in the form of the nanomaterial depending on the organophosphonate. Thus, an OP agent capable of penetrating the basket's cavity to a greater degree affects its shape to trigger the transformation of vesicles into nanoparticles. Moreover, OPs which can insert themselves into the basket's cavity, to a lesser degree, preserve the conical shape of the host such that vesicles only repack into differently sized vesicles. We are currently examining the utility of this well-behaved and stimuli-responsive nanomaterial,<sup>25</sup> with a good affinity ( $K_d \sim \mu\text{M}$ ) toward OPs akin to soman, for the mitigation and detection of toxic nerve agents.

## ■ ASSOCIATED CONTENT

### Supporting Information

Additional details of the experimental and computational protocols. This material is available free of charge via the Internet at <http://pubs.acs.org>.

## ■ AUTHOR INFORMATION

### Corresponding Author

\*E-mail: [badjic.1@osu.edu](mailto:badjic.1@osu.edu).

### Notes

The authors declare no competing financial interest.

## ■ ACKNOWLEDGMENTS

This work was financially supported with funds obtained from the Department of Defense, Defense Threat Reduction Agency (Grant No. HDTRA1-11-1-0042). Computational support from the Ohio Supercomputer Center is gratefully acknowledged.

## ■ REFERENCES

- (1) Kim, K.; Tsay, O. G.; Atwood, D. A.; Churchill, D. G. *Chem. Rev.* **2011**, *111*, 5345–5403.
- (2) (a) Ekstrom, F.; Hornberg, A.; Artursson, E.; Hammarstrom, L.-G.; Schneider, G.; Pang, Y.-P. *PLoS One* **2009**, *4*, e5957. (b) Mercey, G.; Verdelet, T.; Renou, J.; Kliachyna, M.; Baati, R.; Nachon, F.; Jean, L.; Renard, P.-Y. *Acc. Chem. Res.* **2012**, *45*, 756–766.
- (3) Spradling, K. D.; Dillman, J. F. *Adv. Mol. Toxicol.* **2011**, 111–144.
- (4) Dolgin, E. *Nat. Med.* **2013**, *19*, 1194–1195.
- (5) (a) Ajami, D.; Rebek, J. *Org. Biomol. Chem.* **2013**, *11*, 3936–3942. (b) Hargrove, A. E.; Nieto, S.; Zhang, T.; Sessler, J. L.; Anslyn, E. V. *Chem. Rev.* **2011**, *111*, 6603–6782.
- (6) (a) Nachon, F.; Brazzolotto, X.; Trovaslet, M.; Masson, P. *Chem.-Biol. Interact.* **2013**, *206*, 536–544. (b) Otto, T. C.; Scott, J. R.; Kauffman, M. A.; Hodgins, S. M.; diTargiani, R. C.; Hughes, J. H.; Sarricks, E. P.; Saturday, G. A.; Hamilton, T. A.; Cerasoli, D. M. *Chem.-Biol. Interact.* **2013**, *203*, 186–190.
- (7) Sambrook, M. R.; Notman, S. *Chem. Soc. Rev.* **2013**, *42*, 9251–9267.
- (8) Raushel, F. M. *Nature* **2011**, *469*, 310–311.
- (9) Hermann, K.; Ruan, Y.; Hardin, A. M.; Hadad, C. M.; Badjic, J. D. *Chem. Soc. Rev.* **2015**, *44*, 500–514.
- (10) Ruan, Y.; Taha, H. A.; Yoder, R. J.; Maslak, V.; Hadad, C. M.; Badjic, J. D. *J. Phys. Chem. B* **2013**, *117*, 3240–3249.
- (11) Ruan, Y.; Dalkilic, E.; Peterson, P. W.; Pandit, A.; Dastan, A.; Brown, J. D.; Polen, S. M.; Hadad, C. M.; Badjic, J. D. *Chem.—Eur. J.* **2014**, *20*, 4251–4256.
- (12) Chen, S.; Ruan, Y.; Brown, J. D.; Gallucci, J.; Maslak, V.; Hadad, C. M.; Badjic, J. D. *J. Am. Chem. Soc.* **2013**, *135*, 14964–14967.
- (13) Gibb, B. C. *Chemosensors* **2011**, 3–18.
- (14) Chen, S.; Ruan, Y.; Brown, J. D.; Hadad, C. M.; Badjic, J. D. *J. Am. Chem. Soc.* **2014**, *136*, 17337–17342.
- (15) Israelachvili, J. N. *Intermolecular and Surface Forces*; Academic Press: New York, 2011.
- (16) Shimizu, T.; Masuda, M.; Minamikawa, H. *Chem. Rev.* **2005**, *105*, 1401–1443.
- (17) Ghosh, R.; Dey, J. *Langmuir* **2014**, *30*, 13516–13524.
- (18) Sridhar, U.; Pramod, P. S.; Jayakannan, M. *RSC Adv.* **2013**, *3*, 21237–21241.
- (19) Ruan, Y.; Peterson, P. W.; Hadad, C. M.; Badjic, J. D. *Chem. Commun.* **2014**, *50*, 9086–9089.
- (20) Thordarson, P. *Chem. Soc. Rev.* **2011**, *40*, 1305–1323.
- (21) Wittenberg, J. B.; Isaacs, L. *Supramol. Chem. Mol. Nanomater.* **2012**, *1*, 25–43.
- (22) Cram, D. J.; Kaneda, T.; Helgeson, R. C.; Brown, S. B.; Knobler, C. B.; Maverick, E.; Trueblood, K. N. *J. Am. Chem. Soc.* **1985**, *107*, 3645–3657.
- (23) Schneider, H. J.; Duerr, H., Eds. *Frontiers in Supramolecular Organic Chemistry and Photochemistry*; VCH: Weinheim, 1991.
- (24) Yu, G.; Zhou, X.; Zhang, Z.; Han, C.; Mao, Z.; Gao, C.; Huang, F. *J. Am. Chem. Soc.* **2012**, *134*, 19489–19497.
- (25) Ariyadasa, L. W.; Obare, S. O. *Nanotechnol. Environ. Decontam.* **2011**, 347–378.